AD-A114 309 ARIZONA UNIV TUCSON OPTICAL SCIENCES CENTER F/G 20/6
COMPLIANT SURFACES.(U)
APR 82 F A HOPF N00014-81-K-0291
UNCLASSIFIED NL

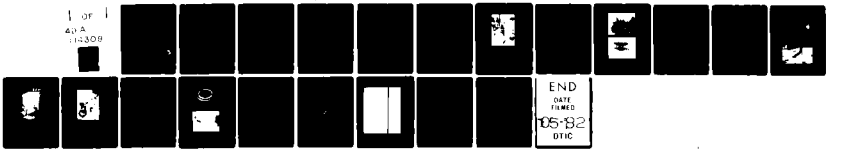

(12)

COMPLIANT SURFACES

F. A. Hopf, Principal Investigator

Optical Sciences Center

University of Arizona

Tucson, Arizona 85721

AD A11

April 1982

Technical Report for Period January 1, 1981 to February 28, 1982

Under Contract N00014-81-K-0291

Prepared for

OFFICE OF NAVAL RESEARCH

Washington, D.C.

UNCLASSIFIED

SECURITY CLASSIFICATION OF THIS PAGE *(When Data Entered)*

REPORT DOCUMENTATION PAGE		READ INSTRUCTIONS BEFORE COMPLETING FORM
1. REPORT NUMBER	2. GOVT ACCESSION NO. AD-A119309	3. RECIPIENT'S CATALOG NUMBER
4. TITLE *(and Subtitle)* Compliant Surfaces		5. TYPE OF REPORT & PERIOD COVERED Technical Report 1/1/81 - 2/28/82
		6. PERFORMING ORG. REPORT NUMBER
7. AUTHOR(s) F. A. Hopf, Principal Investigator		8. CONTRACT OR GRANT NUMBER(s) N00014-81-K-0291
9. PERFORMING ORGANIZATION NAME AND ADDRESS Optical Sciences Center University of Arizona Tucson, AZ 85721		10. PROGRAM ELEMENT, PROJECT, TASK AREA & WORK UNIT NUMBERS
11. CONTROLLING OFFICE NAME AND ADDRESS Office of Naval Research Washington, DC		12. REPORT DATE April 1982
		13. NUMBER OF PAGES 18
14. MONITORING AGENCY NAME & ADDRESS *(if different from Controlling Office)*		15. SECURITY CLASS. *(of this report)* Unclassified
		15a. DECLASSIFICATION/DOWNGRADING SCHEDULE

16. DISTRIBUTION STATEMENT *(of this Report)*

Approved for public release;
distribution unlimited.

17. DISTRIBUTION STATEMENT *(of the abstract entered in Block 20, if different from Report)*

18. SUPPLEMENTARY NOTES

19. KEY WORDS *(Continue on reverse side if necessary and identify by block number)*

Compliant surfaces
Nonlinear optical interferometer

20. ABSTRACT *(Continue on reverse side if necessary and identify by block number)*

The results of experiments on the application of nonlinear optical interferometers to the measurement of compliant surfaces is presented. The interferometer is shown to be suitable for this application. However, the interferometer at 1.06 μm may not be sensitive enough to contour the observed streamwise deformations on the surface. A shorter-wavelength device should be more useful.

DD FORM 1 JAN 73 1473

UNCLASSIFIED

SECURITY CLASSIFICATION OF THIS PAGE *(When Data Entered)*

INTRODUCTION

The objectives of this research were twofold. The first was to establish that nonlinear optical interferometers could usefully contour compliant surfaces under field conditions, and the second was to establish which versions of nonlinear interferometers could be used to contour the streamwise deformations encountered in the NOSC experiments. The two tasks are described separately.

A. EXPERIMENTS ON THE NONLINEAR OPTICAL INTERFEROMETER

The nonlinear optical interferometer is illustrated schematically in Fig. 1 and is described in detail in Ref. 1. The idea is to probe a refractive object with optical wavefronts at the laser (ν_g) and second harmonic ($2\nu_g$) frequencies. Because the index of refraction $n(\nu)$ is a function of frequency, the deformation of the two wavefronts is different inside the refractive medium. At the output, the laser frequency is converted to the second harmonic by means of a suitable crystal and the two second-harmonic beams interfere. The interference fringes occur whenever the wavefronts differ by an integral multiple (m) of a wavelength of the second harmonic (λ_s), i.e.,

$$(n(\nu_f;x,y) - n(2\nu_f;x,y))\,\ell(x,y) = m\lambda_s. \tag{1}$$

Here $\ell(x,y)$ is the physical dimensions of the object as a function of the transverse position x,y where n is also allowed to be a function of transverse position. Let us define the dispersion Δn as

$$\Delta n(\nu_f;x,y) = n(\nu_f;x,y) - n(2\nu_f;x,y).$$

Then the interference fringes occur for

$$\Delta n \ell = m\lambda_s. \tag{2}$$

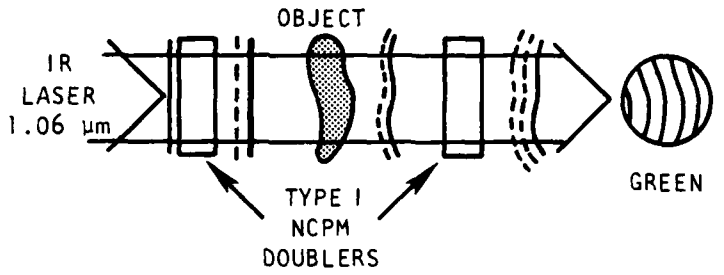

Fig. 1. Schematic of a nonlinear optical interferometer. The optical wavefronts are illustrated by: (___) wavefronts at $\lambda_F = 1.06$ μm; (---) wavefronts at $\lambda_S = 0.53$ μm.

A conventional interferometer causes a wavefront to interfere against a plane wave. Either of the two wavefronts on the left-hand side of Eq. (1) could be used as an object, and interferences occur when

$$n\ell = m\lambda_s.$$

Let us define a distortion $\delta\ell$ such that

$$\delta\ell = \ell_m - \ell_{m-1},$$

where m and m-1 label fringes. Then a conventional interferometer gives a fringe for a distortion $\delta\ell$ such that

$$\delta\ell = \frac{\lambda_s}{n},$$

whereas the nonlinear optical interferometer gives a distortion

$$\delta\ell = \frac{\lambda_s}{\Delta n}$$

between fringes. Since $\Delta n/n$ is usually about 10^{-2}, the nonlinear optical interferometer contours objects whose distortions $\delta\ell$ are the order of 100 λ_s (this is about 0.001 in. or 50 μm). The conventional interferometer is sensitive to deformations on a 1-μm scale (10 μin.). Moreover, a conventional interferometer is sensitive to vibrations, whereas the nonlinear optical interferometer is not.

The key to using nonlinear optical interferometers is the nonlinear crystal that performs the final doubling step. The crystal must perform a faithful reproduction of the incoming laser beam. Such crystals are difficult to find, but a suitable one, which must be held at a fixed temperature, exists for use at the 1.06 μm wavelength of the neodymium:YAG laser. A photograph of the crystal with cooler is shown in Fig. 2. (This crystal was supplied by R. Bocker at NOSC.) The crystal is Y-cut with an aperture of 5 x 5 cm and is held in a copper frame, which is cooled to 15° from the edges. The aluminum block is a heat sink. The temperature tolerances are sufficiently large that a thermometer can be used to set the device to the working temperature.

There are three geometries of interest by which the plastisol sample can be made into a refractive object. These are illustrated in Fig. 3. In Fig. 3a the waves are reflected off the surface of the plastisol. This reflection contours the volume of the water lying between the surface of the tank and the plastisol. In Fig. 3b the object is a combination of plastisol and water held between plane parallel surfaces. Because the plastisol distorts the dispersion of the medium, $\Delta n(\nu_f;x,y)$ is inhomogeneous and can be contoured. Figure 3c is a two-pass version of Fig. 3b, where a reflecting surface is located under the plastisol.

Preliminary Tests

In the first test, we simulated a streamwise groove by cutting a groove 0.001 in. deep and 3/8 in. wide in an aluminum surface. The surface was then buffed to remove small scratches. The object was used primarily for purposes related to part B of this report, but it was also used to illustrate the suitability of the interferometer for the NOSC measurements. In Fig. 4a the object is tested in a Michelson interferometer and in Fig. 4b it is in a nonlinear optical interferometer (the configuration in Fig. 3a is used here and the liquid is ethanol). The gray area in the Michelson interferogram indicates where the groove is, and there is no usable information. In Fig. 4b the fringes are readily visible and agree

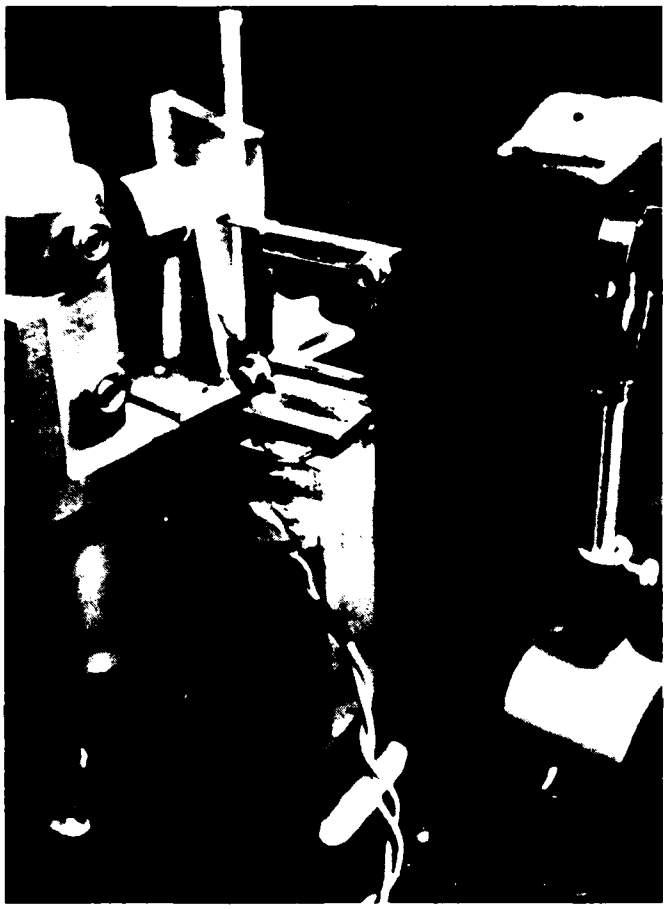

Fig. 2. Picture of $LiNbO_3$ sample. Transparent crystal with 5 x 5 cm^2 aperture is held in copper frame (center). Thermionic cooler holds temperature to a Hg thermometer tolerance. Aluminum stand serves as a heat sink.

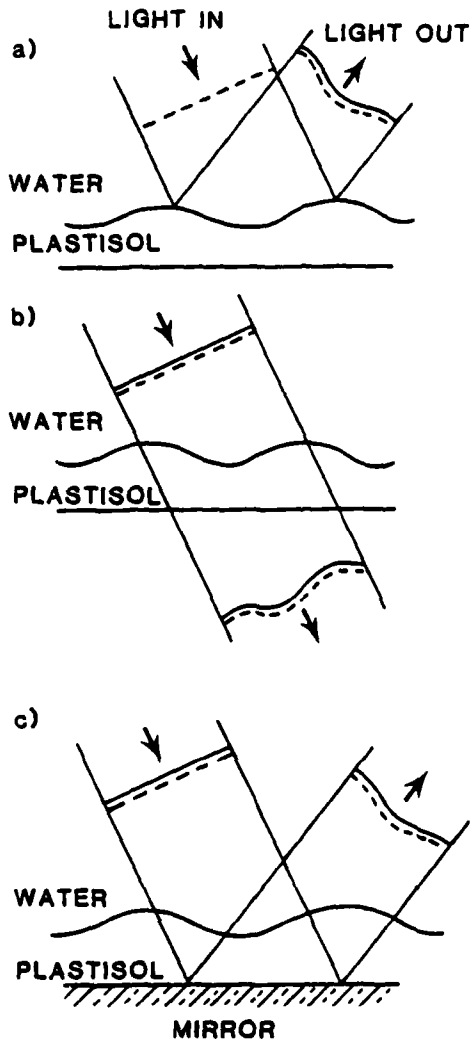

Fig. 3. Schematics of plastisol measurements. (a) Reflection off plastisol surface. Information is a two-pass contouring of the water. (b) Transmission through plastisol. Information is in the single pass contouring of the water-plastisol interface region. (c) Two pass transmission through plastisol. Plastisol is poured over a mirror.

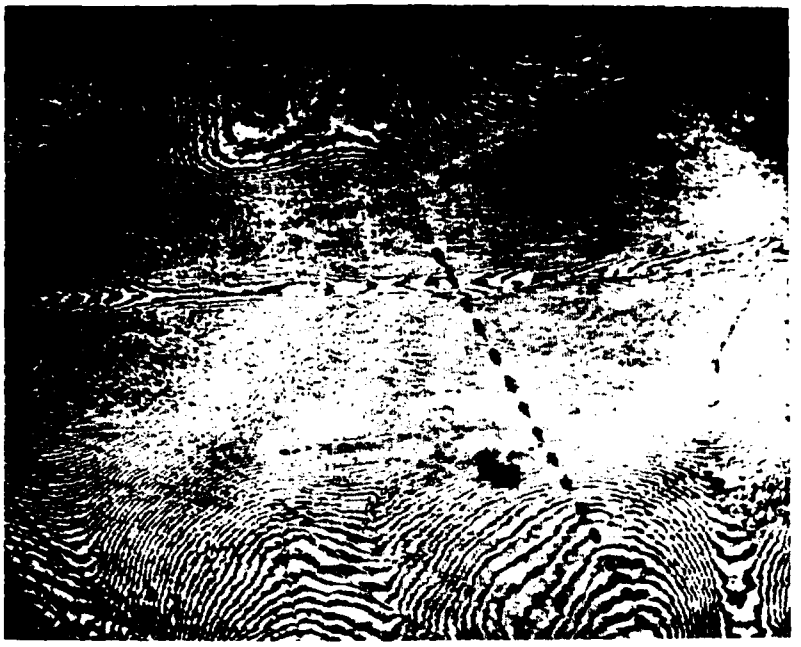

(a)

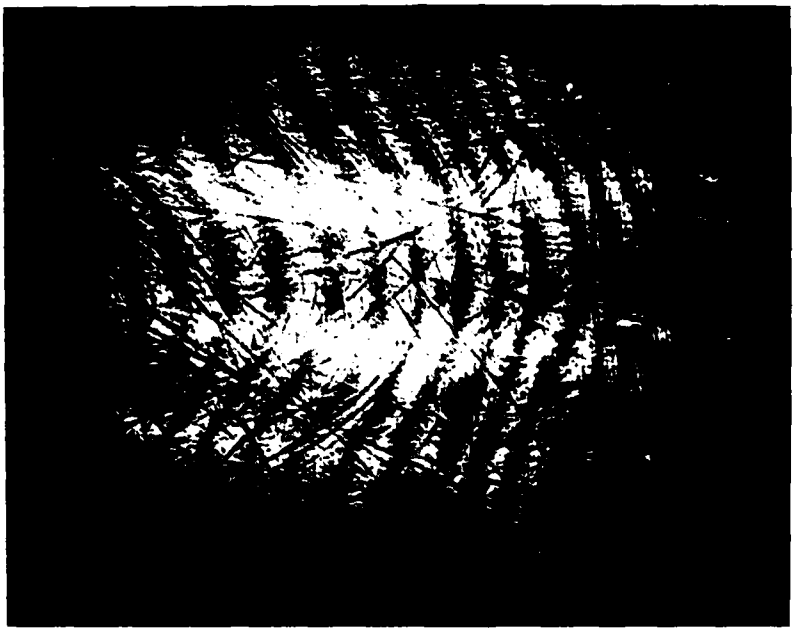

(b)

Fig. 4. Contour of a groove milled in aluminum with dimensions 3/8 in. wide by 0.001 in. deep. (a) Conventional interferometer showing no usable information. (b) Nonlinear optical interferometer showing 1.5 wave distortion over the groove.

with the 0.001-in. estimate of the depth of the groove.

Measurements of the Plastisol

The plastisol can be contoured in any of the configurations of Fig. 3. For the case in Fig. 3a, the reflectivity of the surface needs to be known. For the cases in Fig. 3b and 3c the dispersion relative to that of water is needed. These were measured, and the results are summarized in Table 1. Note, that the sensitivity of each of the configurations in Fig. 4 are summarized in the table.

Of major concern in this measurement is whether the optical properties change under strains. Most materials exhibit strain birefringence, and this would present major obstacles to a successful test using the configurations of Figs. 3b and 3c. We subjected our samples to a wide variety of stresses and found no strain birefringence. As a result we believe that it is highly unlikely that there are significant changes in the optical properties of the plastisol.

Measurements of a Spinning Disk in Water

A number of experiments were performed in a water tank supplied by NOSC. We modified the tank by inserting a wall close to the end of the rotating shaft to minimize the propagation distances. A diagram of the tank and the optical system is given in Fig. 5. Figures 6 through 8 show photographs of the actual setup. Note that the optical system sits on the tank, so it is mechanically coupled to the motor by means of the steel base of the tank. By doing this we demonstrated the capability of acquiring information under realistic and unfavorable field conditions.

Table 1. Optical properties of plastisol and water and the resulting sensitivities ($\delta\ell$ = displacement that causes a shift of one fringe in the interference pattern). Note that the reflectivity R is computed and is of value only as a maximum. Actual reflectivities are sample dependent. The quantity $n_p - n_w$ was measured independently of the measurements of n_w and n_p.

Water:	$n = 1.33$	$\Delta n_w = 0.014 \pm 0.001$
Plastisol:	$n = 1.47$	$\Delta n_p = 0.017 \pm 0.001$
Relative:		$R = 0.25\%$

$$\Delta n_p - \Delta n_w = 0.0040 \quad 0.0005$$

Sensitivity of techniques illustrated in Fig. 3.

(a) $\delta\ell = 0.745$ thousandths of an inch

(b) $\delta\ell = 2.6$ thousandths of an inch

(c) $\delta\ell = 1.3$ thousandths of an inch

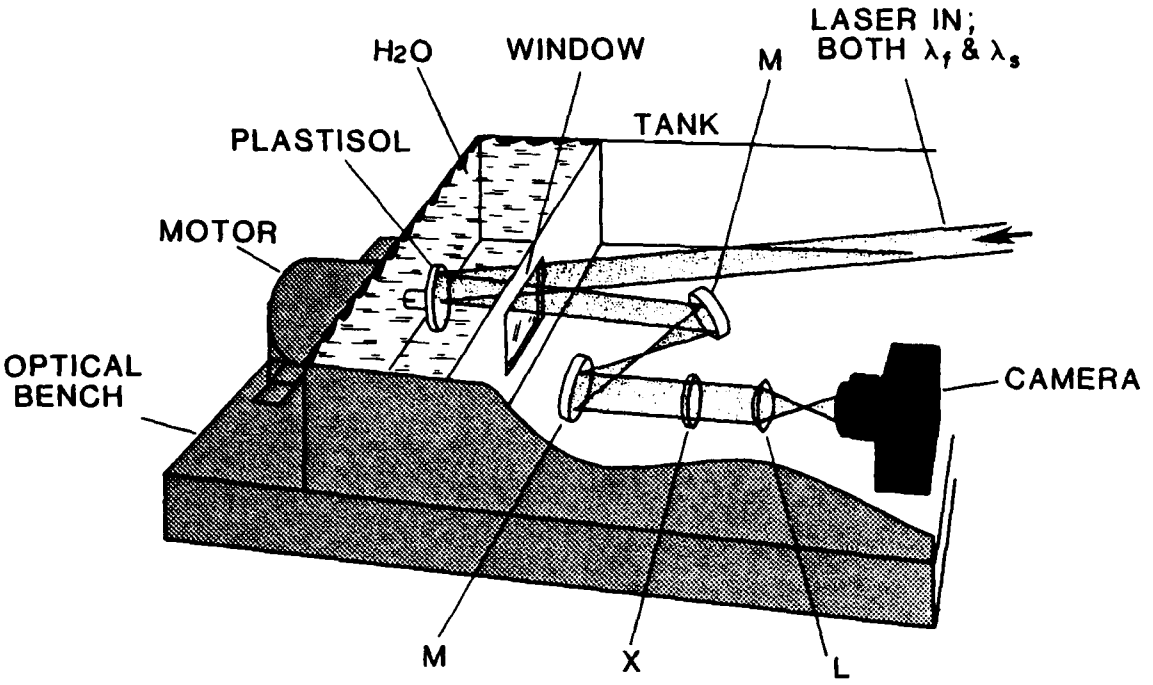

Fig. 5. Diagram of the optical layout and the tank. The wall with a window was inserted to minimize the optical path and the weight. The space was filled with tap water during the experiments. The optical elements are: M, off-axis, parabolic mirrors; X, doubling crystal; L, imaging lens; C, camera.

Fig. 6. Laser used for experiment.

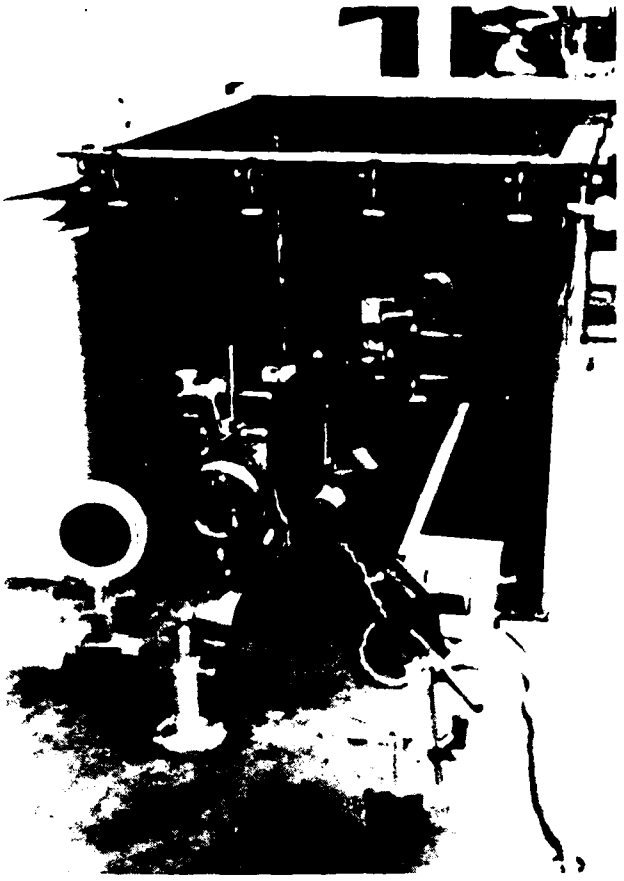

Fig. 7. Tank.

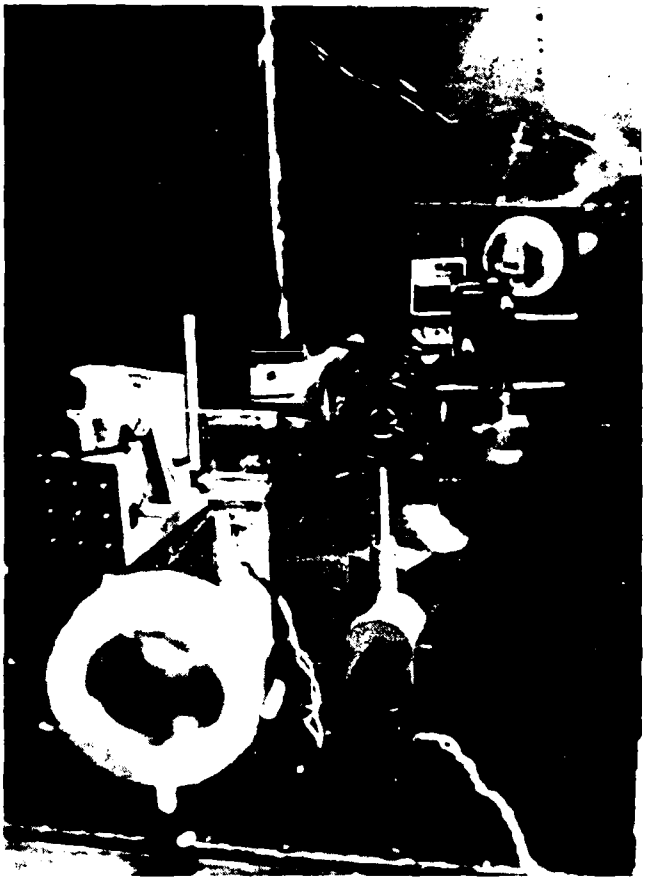

Fig. 8. Closeup of optical system.

Spinning Mirror

Our first tests were made with a mirror glued to the lap. The mirror was spun from 0 to 1100 rpm. At all speeds the interference pattern remained the same. This confirms that (1) turbulent flow in water does not have any effect on optical properties provided the temperature is uniform, and (2) the device is insensitive to vibrations.

Spinning Plastisol

We then spun a sample of plastisol in a Petri dish that was glued to the lap. The mounted sample is shown in Fig. 9. We were able to contour the surface at rest and at low speeds, but not at high rotational speeds. In this test we were using the technique illustrated in Fig. 3a, and the root cause of our difficulty lay in an anomalously rapid deterioration of the plastisol surface, which caused the reflectivity to vanish within a few seconds to a minute (in San Diego the deterioration takes several hours). There are a number of potential causes for this deterioration, but it was not worth the effort to try to find them. This test proved the feasibility of contouring the surface in reflection.

Plastisol Poured over a Mirror

In this test we mounted a mirror inside the plexiglass dish and poured the plastisol over it. Hence we were contouring an object configuration such as that in Fig. 3c. We hoped that this configuration would be more tolerant to surface deterioration and we were correct. The spinning disk does not have streamwise grooves, but does have static divergences, which we were able to contour. An example of the data is given in Fig. 10.

B. PRELIMINARY MEASUREMENTS OF STREAMWISE GROOVES

The measurements made in Part A, particularly the test summarized in Fig. 4 and Table 1, show that the present version of the nonlinear optical interferometer is well suited to the

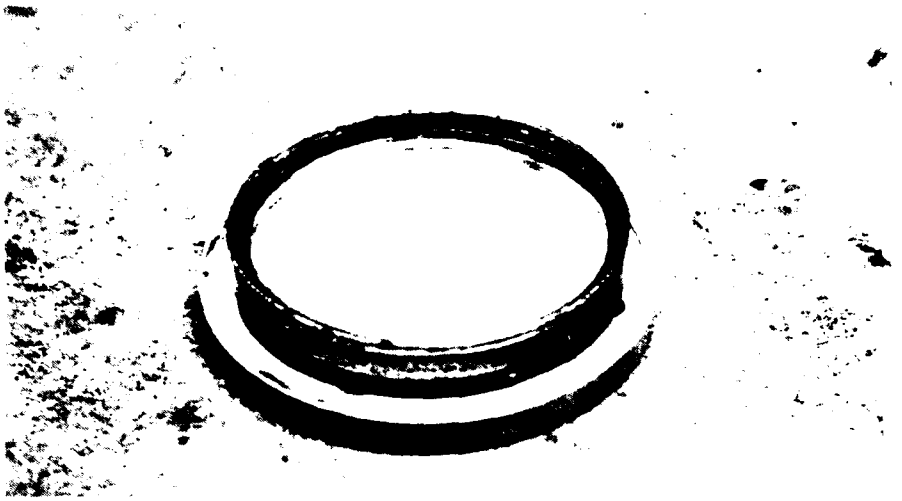

Fig. 9. Plastisol sample.

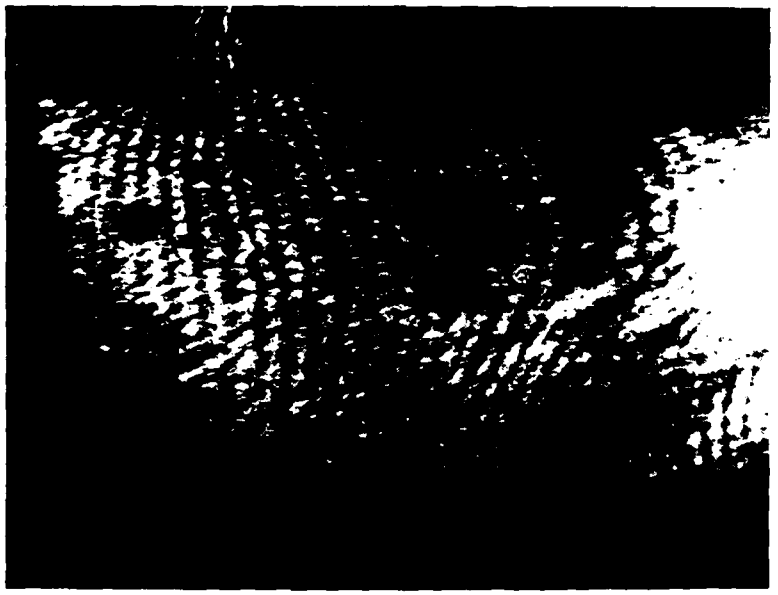

Fig. 10. Example of NLF contour data.

NOSC task if the streamwise grooves are between 0.001 in. and 0.010 in. deep. This was the range indicated by preliminary estimates, but it became clear almost immediately that these estimates are probably wrong. Two tests were developed to clarify the question of how big the grooves should be. Both tests are based on the assumption that the grooves are one dimensional. This hypothesis has been verified by quantitative measurements, but some of the high speed photos of the surface seem to contradict it.

Moving Spot

The goal is to scatter a laser beam off the deforming surface and to track the beam in time. This measurement has already been incorporated into the NOSC apparatus and will not be described here.

This measurement gives information about the speed with which the grooves move and the angular tilts of the surface. In our preliminary measurement with the groove shown in Fig. 4, it was clear that a groove with a width of a few millimeters and a depth of 0.001 in. gives a scattering pattern as it moves that is an order of magnitude wider than that seen in the plastisol. This shows that there is an order of magnitude error in the preliminary estimate of the grooves, and it is possible that they will be so shallow (< 0.00025 in.) that nonlinear interferometers cannot be used.

Line Image

To estimate the depth of a groove from the angle of tilt, it is necessary to measure the width of the groove. A technique for doing this was proposed and tested by us but has not yet been successfully implemented at NOSC. The method consists of regarding the compliant surface as a mirror, and imaging a line source on reflection off this mirror. A preliminary test that we performed is illustrated in Fig. 11, and the data obtained while using the groove in Fig. 4 are shown in Fig. 12. The distortion of the line due to the groove

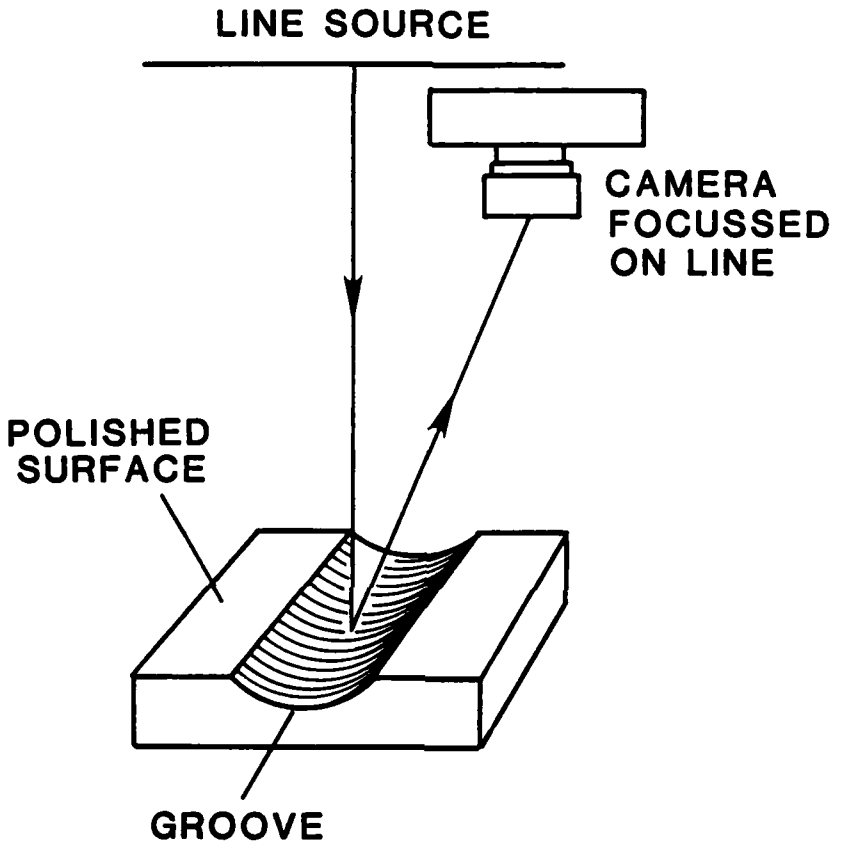

Fig. 11. Line image schematic: camera is focused on line source that is reflected off a polished surface in which there is a groove.

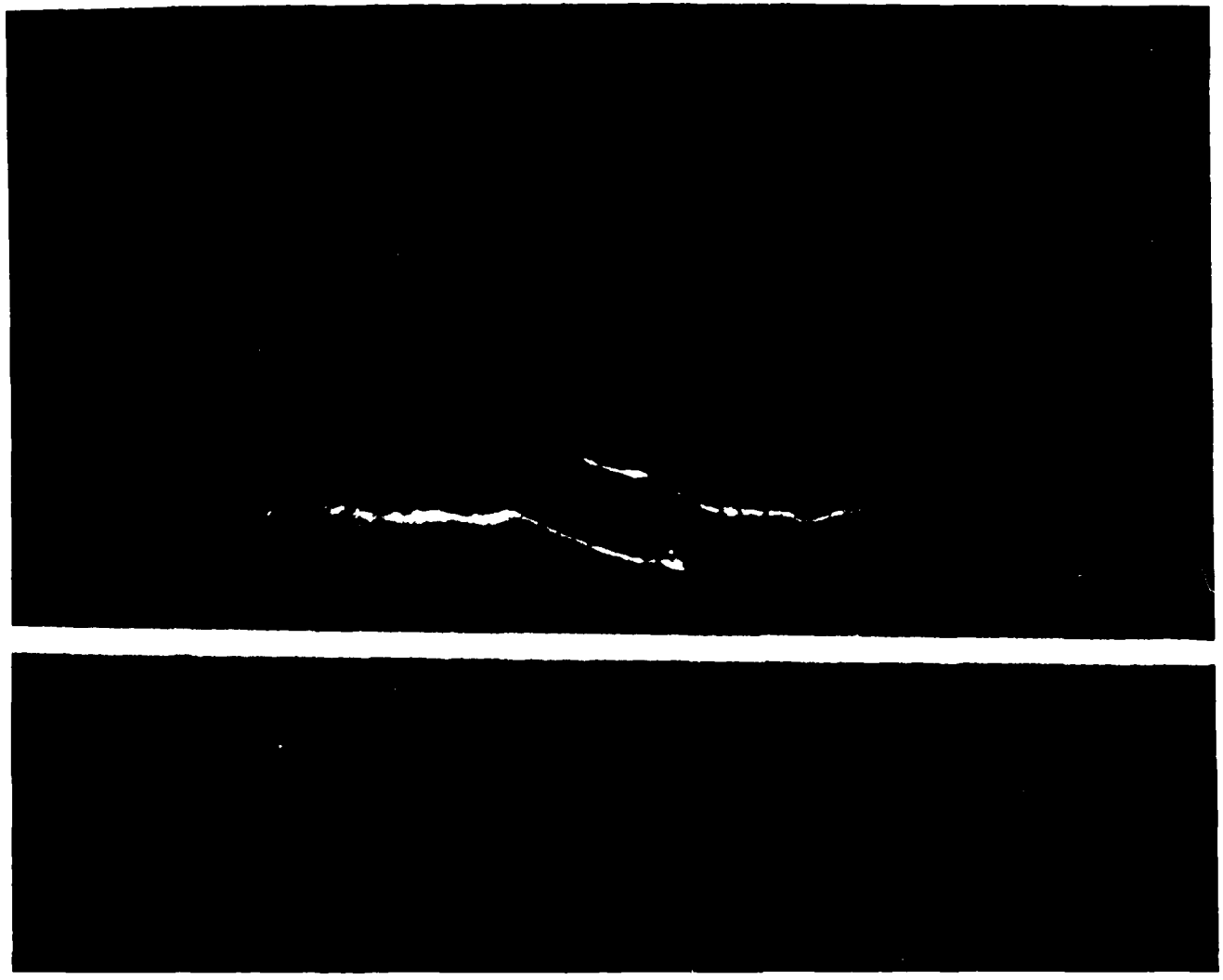

Fig. 12. Data of line image. Line made by He-Ne laser. Dust is blown through laser beam to make it visible. Note: laser is bright and out of focus. Image of laser beam is in tight focus and shows distortion due to groove.

has an "S" shape which gives both the scale and the angles of tilt of the surface. This, combined with the previous test, will be sufficient to design the final optical tests.

SUMMARY

The tests carried out this year show that the nonlinear optical interferometer is well suited for viewing the deformations in a compliant surface. It is not clear whether the streamwise grooves, which are the deformations of interest, are large enough to be usefully contoured with a 1.06 m device. At the present time we are collaborating with NOSC in two directions:

(1) We are trying to measure the scale of the deformation, which will specify adequately what the requirements are for interferometry.

(2) We are developing a nonlinear interferometer at the ruby-laser wavelength that has a greater sensitivity than the YAG device. This will be used, if, as expected, the grooves turn out to have depths in the range of 0.00025 in. to 0.0005 in.

REFERENCES

1. F. A. Hopf, A. Tomita, and G. Al-Jumaily, "Second-harmonic interferometers," Optics Letters 5, 385 (1980).

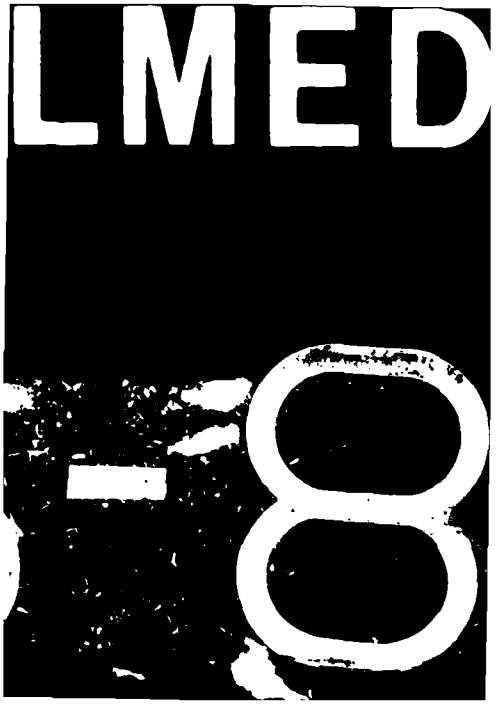
LMED
8